Stott Lowell (Orcid ID: 0000-0002-2025-0731)

Davy Bryan (Orcid ID: 0000-0003-1926-1393)

Shao Jun (Orcid ID: 0000-0001-6130-6474)

Pecher Ingo (Orcid ID: 0000-0001-7397-5069)

Rose Paula, S (Orcid ID: 0000-0001-8109-8641)

Bialas Joerg (Orcid ID: 0000-0001-8802-5277)

CO_2 Release from Pockmarks on the Chatham Rise-Bounty Trough at the Glacial Termination

Lowell Stott[1], Bryan Davy[2], Jun Shao[1], Richard Coffin[3], Ingo Pecher[4],

Helen Neil[5] and Paula Rose[3], Joerg Bialas[6]

[1] Department of Earth Sciences, University of Southern California, 3651 Trousdale Pkwy, Los Angeles, CA 90089.

[2] Department of Marine Geosciences, GNS Science, 1 Fairway Drive, Avalon, Lower Hutt 5010, New Zealand.

[3] Department of Physical and Environmental Sciences, Texas A&M University- Corpus Christi, Corpus Christi, Texas 78412, USA.

[4] School of Environment, University of Auckland, Auckland 1142, New Zealand.

[5] National Institute of Water & Atmospheric Research Ltd (NIWA), 301 Evans Bay Parade, Greta Point, Wellington, New Zealand

[6] GEOMAR Helmholtz-Centre for Ocean Research Kiel, Wischhofstrasse 1-3, 24148 Kiel, Germany

Corresponding author: Lowell Stott (stott@usc.edu)

Key Points:

- Pockmarks of varying size occur across a vast portion of the Chatham Rise and Bounty Trough in the Southwest Pacific
- Pockmarks overlie subsurface deformation features indicative of over-pressurized vertical fluid flow
- Negative $\Delta^{14}C$ anomalies occur in sediments deposited near pockmarks at the glacial termination indicate ^{14}C-dead carbon was released from subducted carbonates.

This article has been accepted for publication and undergone full peer review but has not been through the copyediting, typesetting, pagination and proofreading process which may lead to differences between this version and the Version of Record. Please cite this article as doi: 10.1029/2019PA003674

Abstract

Seafloor pockmarks of varying size occur over an area of 50,000 km^2 on the Chatham Rise, Canterbury Shelf and Inner Bounty Trough, New Zealand. The pockmarks are concentrated above the flat-subducted Hikurangi Plateau. Echosounder data identifies recurrent episodes of pockmark formation at ~100,000yr frequency coinciding with Pleistocene glacial terminations. Here we show that there are structural conduits beneath the larger pockmarks through which fluids flowed upward toward the seafloor. Large negative $\Delta^{14}C$ excursions are documented in marine sediments deposited next to these subseafloor conduits and pockmarks at the last glacial termination. Modern pore waters contain no methane and there is no negative $\delta^{13}C$ excursion at the glacial termination that would be indicative of methane or mantle-derived carbon at the time the $\Delta^{14}C$ excursion and pockmarks were produced. An ocean general circulation model equipped with isotope tracers is unable to simulate these large $\Delta^{14}C$ excursions on the Chatham Rise by transport of hydrothermal carbon released from the East Pacific Rise as previous studies suggested. Here we attribute the $\Delta^{14}C$ anomalies and pockmarks to release of ^{14}C-dead CO_2 and carbon-rich fluids from subsurface reservoirs, the most likely being dissociated Mesozoic carbonates that subducted beneath the Rise during the Late Cretaceous. Because of the large number of pockmarks and duration of the $\Delta^{14}C$ anomaly, the pockmarks may collectively represent an important source of ^{14}C-dead carbon to the ocean during glacial terminations.

1 Introduction

One of the challenges in Ocean and Climate Science is to learn what Earth System processes contributed to the variations in atmospheric pCO_2 that accompanied each glacial cycle of the late Pleistocene. It is particularly striking that each glacial/interglacial cycle during the late Pleistocene was characterized by a long decline of atmospheric pCO_2 that

spanned ~100,000 years but glacial terminations were accompanied by a much more rapid rise in pCO_2. This puzzling temporal asymmetry at the glacial terminations does not match the slow varying changes in solar insolation that seemingly paced glacial cycles at 100,000 year frequency during the late Pleistocene. The saw-toothed shape to glacial cycles and their accompanying changes in atmospheric pCO_2 (Petit *et al.*, 1999) require there to be regulatory mechanisms within the carbon and climate systems that produce theses abrupt transitions.

The leading hypothesis to explain the glacial pCO_2 cycles calls for reduced ocean ventilation during glaciations and accumulation of respired metabolic carbon somewhere in the deep sea (Toggweiler, 1999), followed by rapid ventilation of that stored carbon at glacial terminations, perhaps in response to weakening of the Atlantic Meridional Overturning Circulation (AMOC). In models a weakened AMOC is associated with net transfer of energy from the northern hemisphere to the southern hemisphere. The net transfer of excess energy to the southern hemisphere leads to a reduction of sea ice around the Southern Ocean and perhaps stronger westerly winds (Menviel *et al.*, 2018). The intensification of the westerly winds is key to this hypothesis because it is thought to enhance Ekman pumping and upwelling of deep waters carrying excess carbon to the Southern Ocean (Anderson *et al.*, 2009). But after three decades of scientific inquiry there is still debate about how much excess respired carbon accumulated in the deep-sea during glaciations. There is evidence that the abyssal ocean was more stratified during the last glacial maximum (Adkins *et al.*, 2002; Adkins and Schrag, 2003; Adkins, 2013; Basak *et al.*, 2018; Burke and Robinson, 2012). But these reconstructions do not constrain the rate of ventilation during glacial cycles. Nor do these records constrain the extent to which the deep ocean sequestered additional carbon during glaciations. In fact, radiocarbon measurements from the deep Pacific that span the last glacial maxima do not provide unequivocal evidence that the deep ocean was less ventilated (Broecker *et al.*, 2004; Broecker *et al.*, 2008; Keigwin and Lehman, 2015; Lund *et al.*, 2011).

In a recent assessment of available radiocarbon data from the deep ocean, Zhao et al. (2018) concluded that deep water $\Delta^{14}C$ records do not require basin-scale changes in ventilation rate that would be different from modern, provided there were changes in surface reservoir ages that accompanied the deglaciation. Their study did not preclude the possibility of ventilation rate changes but instead points to the limits of using the available ^{14}C data alone to infer that there were changes in ventilation rate. In another recent study of Neodymium isotope data from the deep Pacific, Hu and Piotrowski (2018) concluded that overturning circulation was actually faster during the glacial relative to the Holocene.

At the same time, there have been recent studies that document large negative excursions in radiocarbon activity ($\Delta^{14}C$) at the last glacial termination (Bryan *et al.*, 2010; Mangini *et al.*, 2010; Marchitto *et al.*, 2007; Ronge *et al.*, 2016; Skinner *et al.*, 2010; Stott *et al.*, 2009; Stott *et al.*, 2019). The spatial and temporal extent of these excursions have not yet been fully constrained, but they are not representative of the ocean's ^{14}C distribution (Zhao *et al.*, 2018). These $\Delta^{14}C$ excursions have thus far been identified at intermediate water depths in the Atlantic, Pacific and Indian Oceans (Bryan *et al.*, 2010; Mangini *et al.*, 2010; Rafter *et al.*, 2018; Sikes *et al.*, 2000; Stott *et al.*, 2009; Stott *et al.*, 2019) and in deeper waters in the south Atlantic (Skinner *et al.*, 2010) and south Pacific, including sites on the Chatham Rise (Ronge *et al.*, 2016). Some studies have called upon these ^{14}C age anomalies as evidence for the release of "old" respired carbon from a formally isolated deep ocean water mass (Bryan *et al.*, 2010; Marchitto *et al.*, 2007; Skinner *et al.*, 2010). Stott and Timmermann (2011) questioned this however, pointing out that the magnitude of the $\Delta^{14}C$ excursions in the Eastern Equatorial Pacific (EEP) are far too large to be indicative of actual ventilation ages. Instead, these excursions are hypothesized to have come from release of geologic carbon from hydrothermal systems nearby (Stott and Timmermann, 2011; Stott *et al.*, 2019), possibly released when temperatures rose and destabilized the CO_2 reservoirs. Other studies

have considered ways for geologic systems to influence carbon cycling on glacial time scales (Broecker *et al.*, 2015; Huybers and Langmuir, 2017; Lund and Asimow, 2011; Ronge *et al.*, 2016). But testing any of these hypotheses is difficult because the observational database is sparse, and the radiocarbon anomalies may involve more than one process. In the present study we present evidence that large $\Delta^{14}C$ anomalies observed in the southwest Pacific on Chatham Rise and Bounty Trough were produced by the release of ^{14}C-dead carbon to the ocean during the last glacial maximum and deglaciation through sea floor pockmarks that overlie subsurface deformation features that are indicative of over-pressured sediments that would have acted as fluid conduits. The radiocarbon anomalies on Chatham Rise and Bounty Trough are found in biogenic sediments deposited directly adjacent to the large pockmarks that occur over a vast portion of the southwestern Chatham Rise and the Bounty Trough (Figure 1). Seismic evidence indicates pockmarks have formed repeatedly during the Pleistocene at a regular recurrence frequency (Davy *et al.*, 2010).

Pockmarks are found on other continental margins as well (Hovland and Judd, 1988). At some of these sites modern pore water geochemistry has been analyzed and found to contain large amounts of methane (Andreassen *et al.*, 2017; Böttner *et al.*, 2019; Feldens *et al.*, 2016) implying that destabilization of methane clathrates at depth resulted in a release of methane that caused the deformation. But at other sites it is less clear what the source of subsurface gas is because direct geochemical measurements from the pockmarks themselves are not available. (e.g. (de Mahiques *et al.*, 2017; Somoza *et al.*, 2014)). In other coastal settings seafloor deformation has been directly attributed to release of He and CO_2 gas from volcanic magmas (Passaro *et al.*, 2016). In the present study we show that on the Chatham Rise geochemical and isotope evidence points to CO_2 rather than CH_4 as the primary gas source responsible for the pockmarks. The most likely source of CO_2 would be from dissociated limestones that subducted beneath the Rise during the Late Cretaceous. Our study

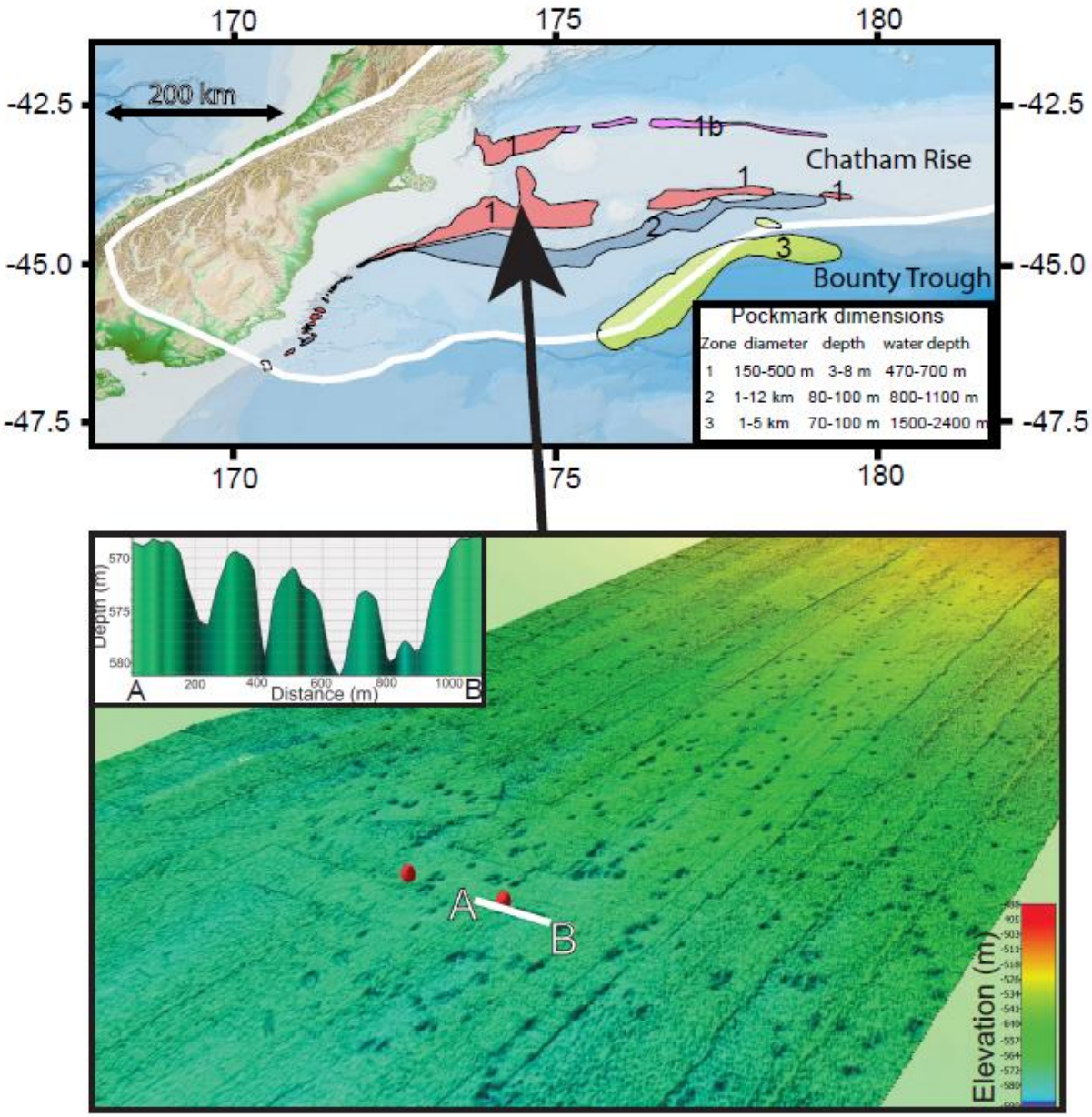

is an initial step in testing the hypothesis that deep sources of CO_2 beneath the Chatham Rise have been released during glacial terminations throughout the late Pleistocene and contributed to the systematic variations in atmospheric pCO_2 that accompanied glacial cycles. If ultimately validated, this hypothesis means that the Chatham Rise acted as carbon capacitor, accumulating carbon during glaciations and releasing carbon to the ocean during glacial terminations.

Figure 1. Upper panel depicts zones where pockmarks of varying size and depth occur across the Chatham Rise and Bounty Trough. Note that the largest pockmarks occur in the Bounty

Trough. The lower panel is a section from Zone 1 illustrating the numerous small pockmarks exposed at the surface. The line A-B (inset) is a section across the smaller pockmarks. The red dots mark locations where piston cores were collected in 2013.

2 Materials and Methods

2.1 SO226 Leg 1, R/V Sonne Geophysical Survey

In an earlier study Davy et al. (2010) hypothesized that the pockmarks spread across the southwestern Chatham Rise were produced by seafloor methane venting from disassociated methane hydrate during glacial terminations. That hypothesis led to a two-leg geophysical and geochemical survey across the southern portion of Chatham Rise in 2013 (R/V Sonne Cruise SO226). Leg 1 of the SO226 Sonne survey undertook a combination of low-fold seismic reflection profiling and 3-D P-cable seismic surveying (at two large pockmark sites). OBS data were collected for velocity control. The survey also collected Parasound sub-bottom seismic data and multibeam data for seafloor mapping.

2.2 SO226 Leg 2, R/V Sonne Coring and Geochemical Survey

Coring operations during SO226 Leg 2 targeted sites identified using seismic data from Leg 1 and included both piston and multi coring (Figure 2). Multi-cores were between 8 and 42 cm long and were sectioned at 1 cm intervals. Each core was split into ~ 25 sections at 10-40 cm intervals and capped. Porewater was extracted from each section using rhizon samplers (Dickens *et al.*, 2007; Seeberg-Elverfeldt *et al.*, 2005). Porewaters were extracted onboard for analysis of sulfide, sulfate, chloride, and dissolved inorganic carbon (DIC) concentrations. Samples were also preserved for stable carbon isotope ratios of DIC (Coffin,

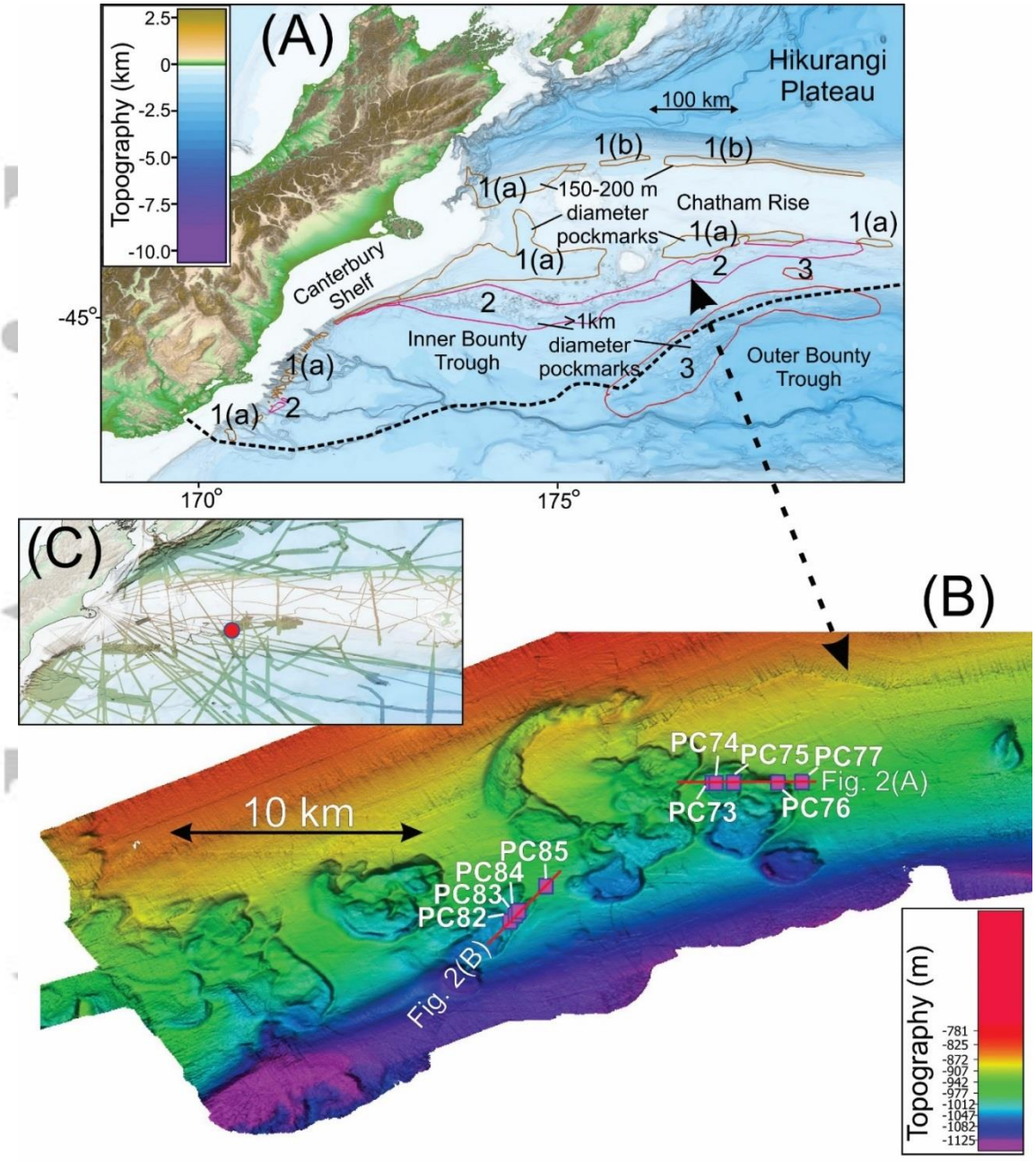

Figure 2. Upper panel (A), location of pockmarks over bathymetry (courtesy of NIWA). Heavy dashed line marks the interpreted southern extent of Hikurangi Plateau flat-subduction (Davy, 2014). Lower panel (B) multibeam bathymetry image from survey SO226 with core locations (red boxes). Red dot in panel (C) shows the profile lines and the location (red dot) of the pockmarks and cores shown in panel (B). Red dot in panel (C) covers the extent of panel (B).

2014). The onboard porewater analysis was used to assess whether there is a modern flux of methane affecting the pore water chemistry (Coffin, 2008).

For radiocarbon isotope **a**nalysis, background radiocarbon shipboard wipe tests were conducted to determine levels of radiocarbon present in laboratories, work and storage areas and in the portable lab van (Coffin *et al.*, 2013b). The piston core PC75 $\Delta^{14}C$ and stable isotope data are from Shao et al (2019). The bulk sediment ^{14}C ages for piston cores PC45 and PC54 were generated at the Rafter AMS lab in New Zealand (Supplemental Table S1). For radiocarbon isotope analysis of bulk sediment carbonate, CO_2 was generated by acidification and sealed tube (Coffin *et al.*, 2015). Sample and data processing are as described by Stuiver and Polach (1977). The blank corrected, fraction modern was normalized to $\delta^{13}C$ = -25‰ defined by Donahue et al. (1990). Stable carbon isotope analyses were combined with radiocarbon data to assess if there has been methane oxidation (Coffin *et al.*, 2015). Stable oxygen and carbon isotope data from foraminifers from piston core PC75 are from Shao et al (2019).

2.3 Age Modelling and $\Delta^{14}C$ Reconstructions.

We recalculated $\Delta^{14}C$ for the Ronge et al. (2016) cores, PS75-100-4 and SO213-82-1 from the Bounty Trough as well as the PS75-104 and SO213-84-1 cores from the Chatham Rise based on a new age model developed using BChron. We did this so that all of the core chronologies are derived using the same calibration curve (MARINE13). For the late glacial and early deglacial sections we adopted their surface reservoir ages because they are within ~300 years of that used by Shao et al. (2019). There is one exception; in Ronge et al's "tuned" age model for the PS75-104-1 core, the authors estimated a surface reservoir age of 243 years at 96cm (15,435 ^{14}C age). We are not able to assess how robust either reservoir age is for this time interval. But importantly, in the early deglacial and late glacial portions of both cores the $\Delta^{14}C$ estimates are in close agreement and both cores document large negative $\Delta^{14}C$ excursions at shallow intermediate water depth on the Chatham Rise (Figure 5). The

estimated uncertainties arising from both the $\Delta^{14}C$ estimates and age uncertainties are plotted as slanted quivers.

2.4 Earth System Modelling.

The cGENIE model includes a 3-D dynamical ocean model coupled to the 2-D energy-moisture balance atmospheric model (Edwards and Marsh, 2005). The ocean model is based on a 36x36 horizontal grid with 16 vertical layers. cGENIE has a dynamic and thermodynamic component of sea ice. The model also incorporates a marine biogeochemical cycling of carbon and other tracers (Ridgwell *et al.*, 2007). cGENIE simulations were first run under pre-industrial conditions (Cao *et al.*, 2009) for 10,000 years, with prescribed atmospheric pCO_2 = 278 ppm and atmospheric $\Delta^{14}C$ = -1‰. Then the model was further spun up for 50,000 years with an atmospheric ^{14}C production rate of to 350 mol/yr, equivalent to 1.3 atoms/cm^2/s. The atm $\Delta^{14}C$ could evolve freely at this stage. At the end of 50,000 years, atmospheric $\Delta^{14}C$ = 0.8‰. The spin-up is not an attempt to reproduce the atmospheric radiocarbon condition at ~30kyrBP, when Ronge et al (2016) hypothesized mantle sourced carbon was released into the South Pacific. For example, a production rate of 1.3 atoms/cm^2/s that we used is much smaller rather than ~2.2 atoms/cm^2/s from a recent reconstruction (Hain *et al.*, 2014). This is mainly because the total carbon inventory in the atmosphere-ocean system in cGENIE is ~36,000PgC and the bulk $\Delta^{14}C$ at equilibrium is -180‰, while in the calculation by Hain et al. (2014), the total carbon inventory is 43,000 PgC and bulk $\Delta^{14}C$ is ~0‰ at 30kyrBP. The smaller total carbon inventory and more negative bulk $\Delta^{14}C$ in our spin up leads to a smaller ^{14}C rate compared to Hain et al., (2014) and therefore, requires a smaller production rate at equilibrium. Nonetheless, our goal here is to achieve an ocean and atmosphere ^{14}C field that is in equilibrium with the prescribed ^{14}C production rate and therefore we can be sure that the ^{14}C response in the sensitivity experiments is not caused by

the ^{14}C production rate in the atmosphere. In the DIC injection experiments, atmospheric ^{14}C production was held constant. The rationale for this is that there is no trend in the reconstructed atmospheric ^{14}C production rate between 30-20kyrBP (Hain *et al.*, 2014).

In each sensitivity experiment, a brine rejection process was turned on in cGENIE. The brine rejection is a simple parameterization of the sink of very salty water in the Southern Ocean during sea ice formation. The strength of this mechanism is represented by the "frac" parameter in cGENIE. The "frac" parameter is the proportion of the rejected salt that sinks to the abyss in the Southern Ocean. The higher the "frac", the denser and thus more stratified, the deep ocean becomes. A 'frac' value of 0.6 was chosen, falling in the range of a previous work that attempted to fit the simulated deep ocean radiocarbon to the reconstructions using the CLIMBER-2 model (Mariotti et al., 2013).

For injections of 0.16, 0.32, 0.64 and 1.28 GtC/yr over 10,000 years, the total amount of carbon released is 1600, 3200, 6400 and 12800 GtC, respectively. This extra carbon would have a significant effect on the Earth's radiation budget and consequently, a strong influence on the simulated climate. To compare the direct $\Delta\Delta^{14}C$ response driven by different injection rates in these sensitivity experiments we therefore fixed the radiative forcing in all simulations to be 60% of the pre-industrial level (i.e. LGM-like). Again, the purpose is to assess how the radiocarbon anomalies are manifest in the ocean in response to a release of carbon from the EPR, not to accurately simulate the climate system response to that carbon release.

3 Results

3.1 Large Pockmarks and Fluid Conduits on the Chatham Rise

Numerous pockmarks of varying size are documented over >50,000 km^2 of the Chatham Rise, Canterbury Slope and Inner Bounty Trough, New Zealand (Figure 1).

Multibeam data collected post 2010 greatly extends the distribution of seafloor depressions (pockmarks) documented in earlier surveys (Davy *et al.*, 2010). Smaller pockmarks, 150-500 m wide and 3-8m deep, occur at water depths between 500 and 700m. Larger pockmarks, 1-7 km in diameter and 80-100 m deep, occur in 800 to1100m water depths (Figure 1). There are numerous large, 1-5 km diameter (100m deep) pockmarks on the southern margin of the plateau. There are also several giant pockmarks that are up to 12km in diameter. At water depths of 1500-2400m, across the inner-outer Bounty Trough boundary, there are pockmarks 1-5 km in diameter and 70-100m deep (Figure 1, Figure S1).

Echosounder images from the north-western part of the study area also identify numerous buried pockmarks formed on surfaces with high-amplitude reflections (Figure 3). With the recent development of high resolution (better than 1ms two-way travel-time and 1m depth vertical) sub-bottom profilers that can penetrate up to 100 m in soft sediment, the pattern of glacial deposition becomes recognizable (Bull *et al.*, 2006; Davy *et al.*, 2010). Alternating banding in the seismic image (Figure 3) is attributed to glacial/interglacial cycles that affected the percentage of terrestrial input (80% carbonate during warm inter-stadial periods versus <25% during glacials (Carter *et al.*, 2000). We infer that the "darker" (high-amplitude reflections) horizons represent the higher-density terrestrial input during full glacials (Red arrows in Figure 3B). Sedimentation rates in the region of this seismic section (Carter *et al.*, 2000) are consistent with this interpretation (Davy *et al.*, 2010) and provide the only plausible mechanism in agreement with the observed regional sedimentation cycles. Small pockmarks, approximately the size of the seafloor pockmarks (Figure 1), are also visible along these high-amplitude horizons. The pockmarks appear to have formed initially only at these horizons, which we interpret to mark glacial terminations (occurring every ~100,000 years). Pockmark morphology may persist in some instances until the next glacial

termination and we postulate these pockmarks have been a focus for repeated fluid venting at glacial terminations (Davy *et al.*, 2010).

The origin of these pockmarks on the Chatham Rise and Bounty Trough has long been a mystery. Seafloor pockmarks have been attributed to sudden release of fluids or gas (Hovland and Judd, 1988; Hovland *et al.*, 2002). And in an earlier study it was hypothesized that the Chatham Rise pockmarks formed in response to destabilization of methane clathrates (Davy *et al.*, 2010). The coincidence between the upper limit of shallow pockmarks and the top of methane gas hydrate stability in the ocean led to the hypothesis that pockmarks formed from methane gas hydrate dissociation at or near the glacial terminations following depressurization associated with sea-level lowering. However, a subsequent geochemical

survey of porewater sulphate, methane, sulfide and dissolved inorganic carbon profiles (Section 3.2) found no evidence of methane.

An alternative mechanism proposed for the formation of small, shallow pockmarks

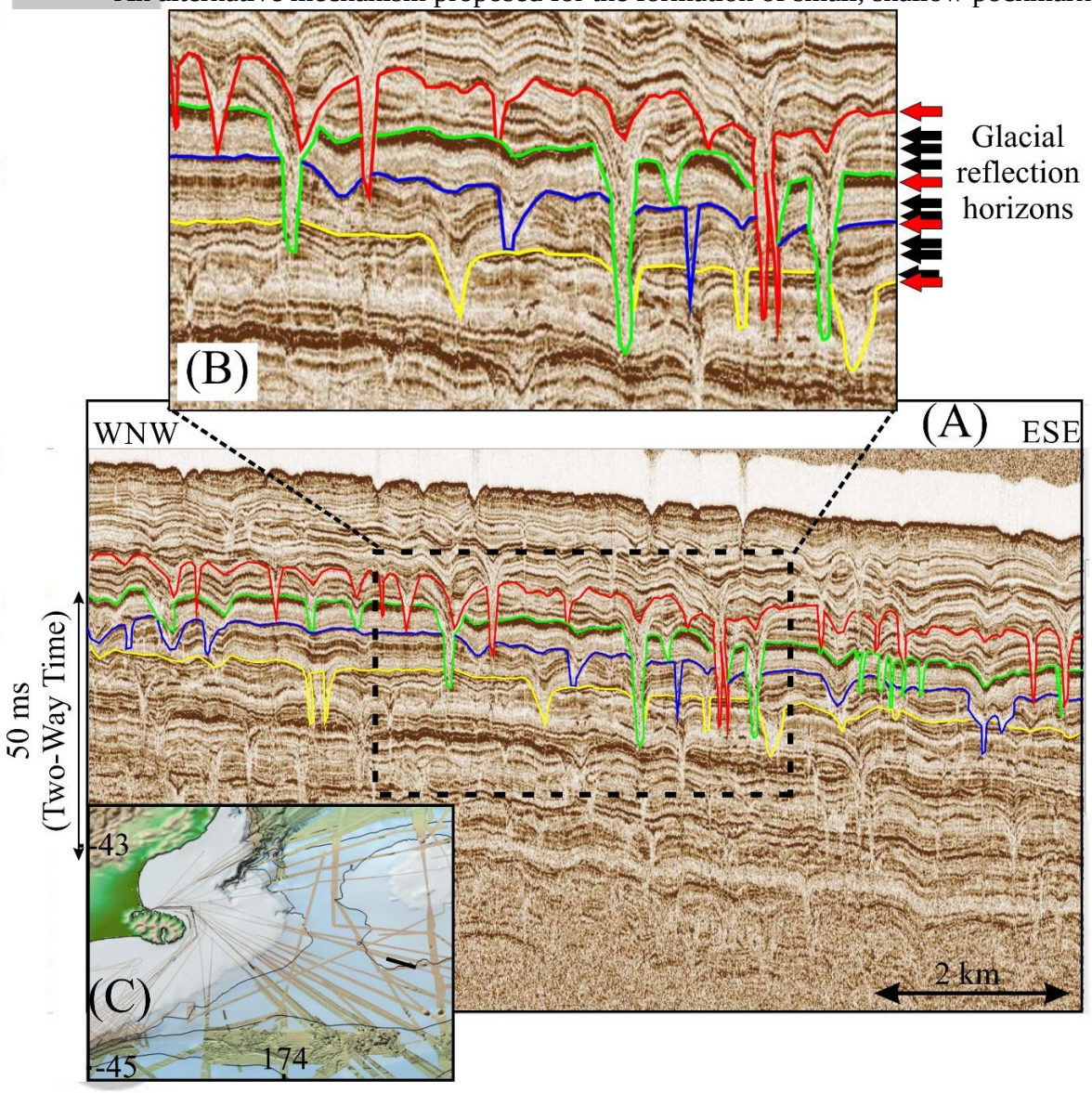

Figure 3. (A) A high-resolution sub-bottom PARASOUND profiler image of small pockmarks, 2-3 m deep and 100-200m wide, characteristic of pockmarks throughout the southwestern Chatham Rise area - in Zone 1 (Figure 1). Inset (B) highlights that the pockmarks are only occurring on top of every fourth stadial cycle (Red arrows). (C) Map of swath multibeam coverage with the black line highlighting the location of seismic profile (A). Parasound data is from R/V Sonne survey ANT26_3 (Gohl, 2003).

along the western edge of the Canterbury Basin called upon groundwater flow through canyon walls induced by the Southland current (Hillmann et al., 2015). However, it is

difficult to explain the wide-spread occurrence of pockmarks across the Chatham Rise with this model, particularly in deeper waters.

A polygonal fault system appears beneath the pockmark fields in the 3-D seismic data that is indicative of significant dewatering (Cartwright and Lonergan, 1996; Hillman *et al.*, 2015; Klaucke *et al.*, 2018; Waghorn *et al.*, 2018) It is conceivable therefore that water released from the compacting mudstones associated with the polygonal faulting could have facilitated some of the sea floor depressions. However, Hillman et al. (2015) could not establish any correlation between seafloor pockmarks and individual polygonal faults in data from the western Canterbury Basin

With widespread identification of Eocene-Miocene polygonal faulting in seismic data, Klaucke et al (2018) suggested dewatering from opal A/CT transformation would cause the faults to act as fluid pipes. These authors proposed, that as fluids escaped from the faults at the seafloor, that scouring by bottom currents formed the seafloor depressions or pockmarks. The widespread presence of polygonal faulting observed over the Chatham Rise and within the Bounty Trough supports a compactional phase change and the release of water, whether from the opal-A/CT transition or the transition of calcareous ooze to chalk. However, this model does not account the large conduit structures we document beneath the pockmarks (Figure 4), nor the recurrence frequency of shallow pockmarks at glacial time scales (Davy *et al.*, 2010). There is also no special correlation between shallow pockmarks and underlying

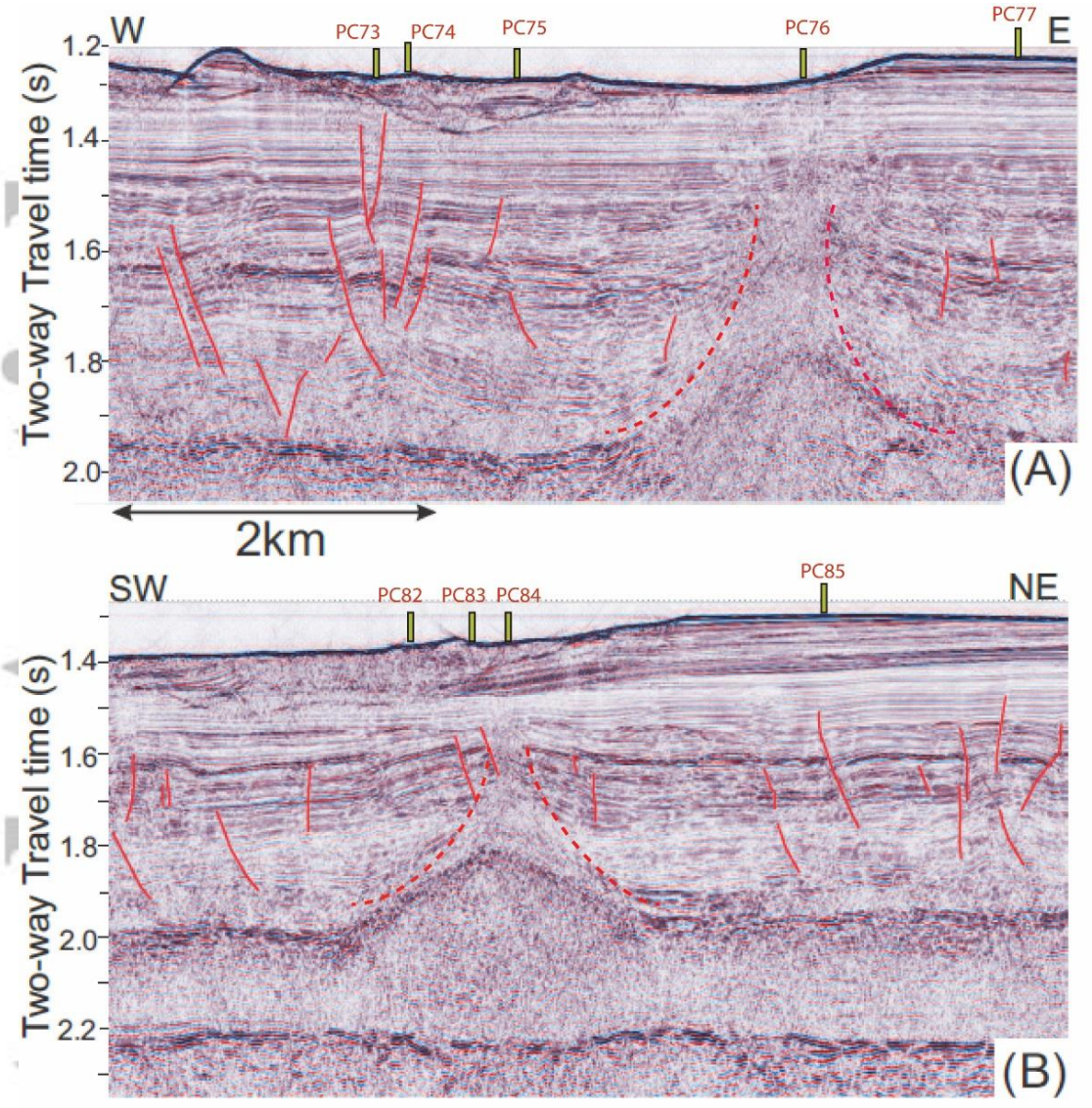

Figure 4. Seismic sections extending through piston core sites shown in Figure 1. The red dashed lines mark approximate boundaries of fluid-flow features ('vent conduits'). The solid red lines delineate the location of listric faults. Also shown are the location of piston cores (PC) collected during the 2013 expedition.

polygonal faults. At the same time, these early Cenozoic fault networks may have facilitated the more recent release of fluids from near basement.

We present recently acquired geophysical evidence that the large pockmarks are associated with deeply rooted paths of fluid and gas migration. Seismic profiles above pockmarks on the Chatham Rise reveal numerous subsurface structures that are indicative of near-vertical gas and fluid migration (Figure 4). The most prominent of these features are termed 'vent conduits' because they lie directly beneath the large pockmarks (>1km

diameter) and provide a conspicuous pathway for fluid and gas migration to reach the seafloor. Elsewhere above the subducted Hikurangi Plateau (Figure 4) upward fluid migration along faults is also evident. At the boundary between the inner and outer Bounty Trough pockmarks occur above the highly faulted eastern edge of the subducted Hikurangi Plateau (Figure 1) (Davy, 2014). These faults would also act as pathways for upward fluid migration. In the seismic cross-section (Figure 4A) listric faults and adjacent rotated sedimentary layers below core PC73 (Figure 4A) are characteristic of an extensional depositional environment. Such faults are likely an expression of Eocene polygonal faulting that would have facilitated upward fluid migration (Waghorn *et al.*, 2018). Further to the east the sedimentary layers at 350-700m below the seafloor are curved upward around a junction point more-or-less directly beneath the PC76 core (Figure 4). The conical shaped features seen in the 2D seismic sections (Figure 4), is characteristic of buoyancy-driven fluid and fluid-mobilized sediment flow (Waghorn *et al.*, 2018). Subsurface vent conduits like those shown in Figure 2 are also observed beneath other large pockmarks across the southwest Chatham Rise.

3.2 Geochemical Assessment of Modern and Past Methane Fluxes

To evaluate whether methane could be a primary source of gas beneath the pockmarks the vertical methane flux and its spatial variation was investigated by analyzing sediment porewaters for anaerobic methane oxidation (Coffin *et al.*, 2008; Coffin *et al.*, 2013a; Coffin *et al.*, 2015; Coffin, 2014). The decline in sediment methane and porewater sulfate concentrations, associated with increased porewater dissolved inorganic carbon and sulfide, was used to identify a depth of the sulfate-methane-transition depth (SMT) and used as a proxy for vertical methane migration. Sediment porosity and sulfate profiles provide an annual vertical methane flux. This analysis was conducted on board to provide continuous comparison with the seismic data. The porewater data from piston cores PC75 and PC83

were taken during the 2013 SO226/2 expedition. Tables S2 and S3 and Figures S3 and S4 summarize the porewater sulfate (SO_4^{-2}), methane (CH_4), dissolved inorganic carbon (DIC) and the stable carbon isotope ($\delta^{13}C$) results for porewater profiles from these cores. Several observations confirm that there is no vertical migration of methane at these locations; 1) Low background CH_4 concentrations, near the limits of detection at all locations; 2) The vertical profiles show deep CH_4 concentrations declining while DIC increases proportionally with SO_4^{-2}. In this study there was no relation between SO_4^{-2} and CH_4. SO_4^{-2} was uncharacteristically high throughout the cores. In an active CH_4 flux region SO_4^{-2} typically disappears from porewater in the top 100 cm (Coffin, 2008). Anaerobic oxidation of CH_4 in porewaters produces an increase in DIC concentration and the $\delta^{13}C$ of DIC becomes strongly depleted. No such geochemical trend was observed and the moderate $\delta^{13}C$ DIC change suggests there has been shallow organoclastic sediment carbon cycling, but no methane oxidation.

We cannot exclude the possibility that methane has, in the past, contributed to the flux of fluids from the subsurface structural features. But over the course of the past 25ky (the length of our core records), the benthic $\delta^{13}C$ stratigraphy from available piston cores does not contain any anomalously low values. In fact, the PC75 benthic $\delta^{13}C$ stratigraphy documents a positive excursion during the deglaciation when the $\Delta^{14}C$ values exhibit a negative excursion (Figure 5). Sikes et al (2017) found a similar positive $\delta^{13}C$ excursion in another core (79JPC) taken at similar water depth from the Bay of Plenty.

3.3 Evidence of ^{14}C-depleted Fluids Entering the Ocean from Subsurface Reservoirs Beneath Chatham Rise at the Glacial Termination

The uppermost sediments at the PC75 core site are undisturbed. The planktic and benthic $\delta^{18}O$ stratigraphies from this core document continuous sediment accumulation since

the last glacial maximum (Figure 5). The radiocarbon ages obtained for both planktic and benthic foraminifera from this core were converted to radiocarbon activity ($\Delta^{14}C$) (Figure 6).

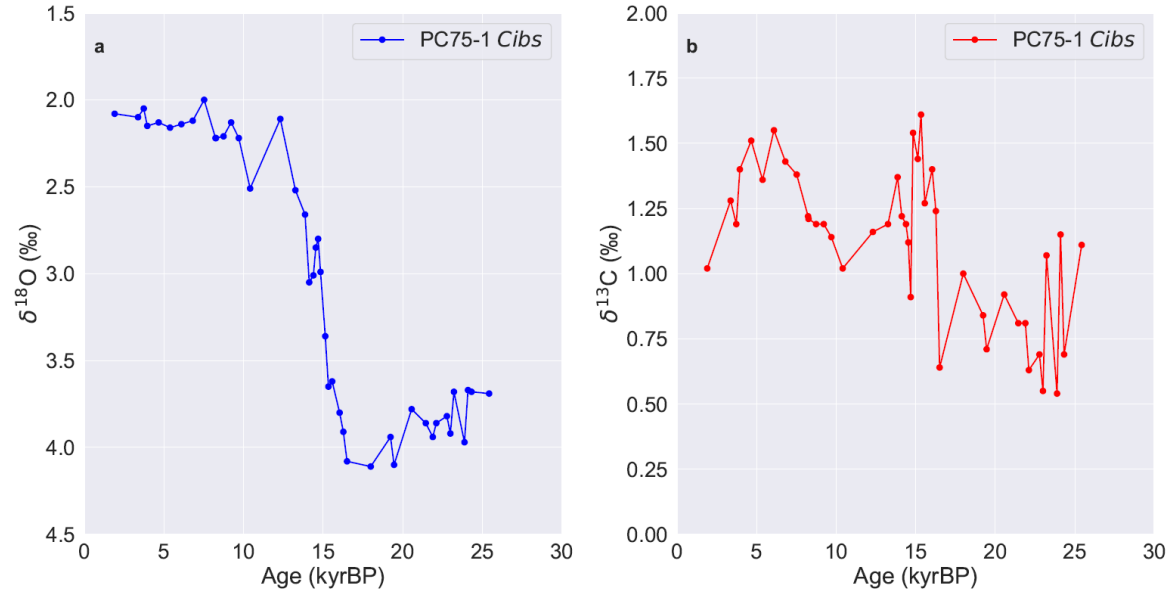

Figure 5. a) PC75-1 benthic $\delta^{18}O$ stratigraphy; b) PC75-1 benthic $\delta^{13}C$ stratigraphy. There is no evidence of a negative $\delta^{13}C$ excursion during the last glacial termination as would be expected if the source of carbon responsible for the large $\Delta^{14}C$ excursions came from either mantle-derived CO_2 or from methane.

Today, the PC75 core location is bathed by well-ventilated, relatively 'young' AAIW. The $\Delta^{14}C$ offset between AAIW and the atmosphere today is ~100-150‰. During the late glacial and in the early deglacial however, the benthic-Atmospheric $\Delta^{14}C$ offset ($\Delta\Delta^{14}C$) at the PC75 site increased to ~400‰ (Figure 6). Ronge et al.'s PS75-104 and SO213-84-1 record documents similar values (Figure 6) to those of PC75. At deeper water depths, between 2000 and 2500m, the $\Delta\Delta^{14}C$ offset between Pacific Deep Water and the atmosphere today is ~200‰, reflecting the fact that Pacific Deep Water is older and has acquired respired carbon along its path from the North Pacific to the Southern Ocean. In the sediment cores from the Bounty Trough analyzed by Ronge et al (2016) the benthic-atmosphere $\Delta\Delta^{14}C$ values during the late glacial and early deglacial increased to ~1000‰ (Figure 5). Sikes et al, (2000) also found similarly ^{14}C-depleted values in association with Kawakawa tephra in a core not far from Ronge et al's core in the Bounty Trough (Figure 6). Each of these cores is

located close to large pockmarks that occur within the Bounty Trough (Figure 1). It appears from these records that highly ^{14}C-depleted values were recorded across a wide range of water depths and across the Chatham Rise and Bounty Trough beginning at approximately 25kyBP, in close temporal association with the Kawakawa tephra. But similarly depleted values are not observed in the intermediate depth cores from the Bay of Plenty to the north of the Chatham Rise (Rose *et al.*, 2010; Sikes *et al.*, 2016).

Table 1.				
Core	Long.	Lat.	Depth (m)	Author
PS75-104-1	-185.5	-44.77	835	(Ronge *et al.*, 2016)
SO213-84-1	-185.4	-45.13	972	(Ronge *et al.*, 2016)
PS75-100-4	-182.9	-45.76	2498	(Ronge *et al.*, 2016)
SO213-82-1	-183.4	-45.78	2066	(Ronge *et al.*, 2016)
U938	-180.5	-45.1	2700	(Sikes *et al.*, 2000)
PC75-1,2	-182	-44.24	967	This paper

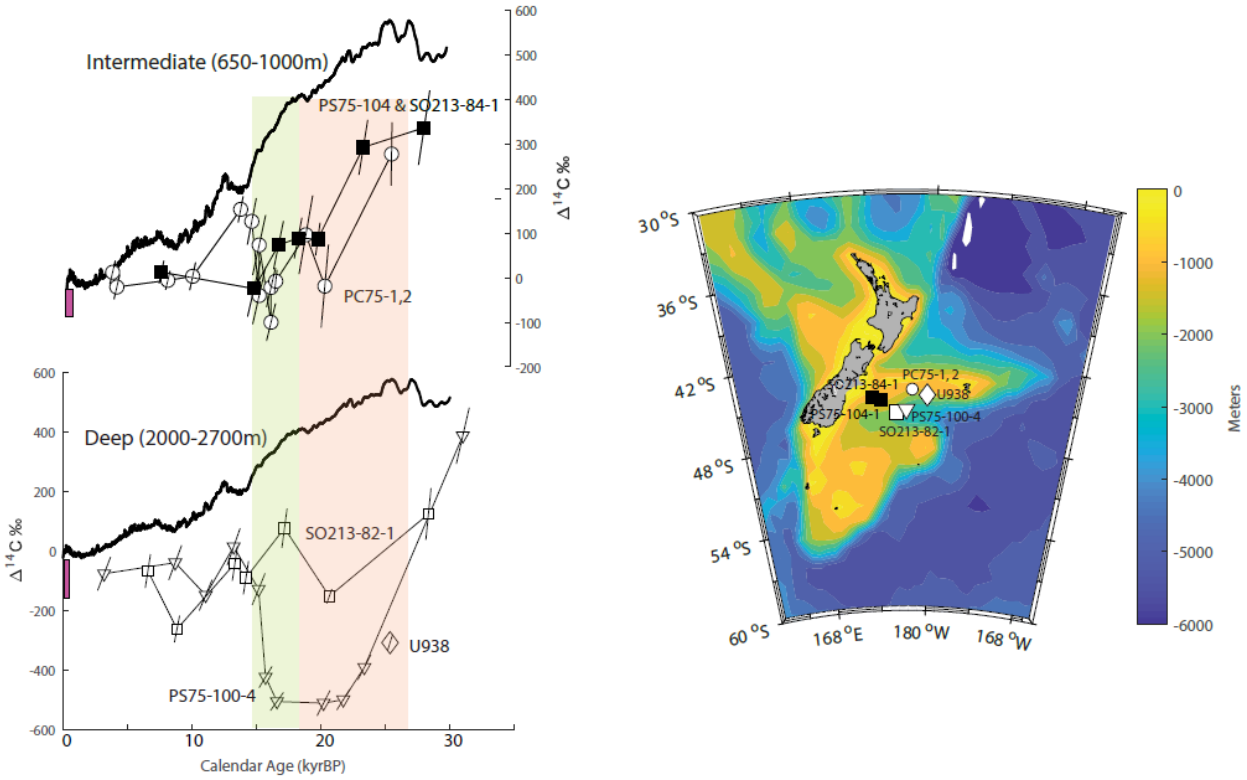

Figure 6. Left panel, $\Delta^{14}C$ for the atmosphere (INTCAL13, black solid lines), shallow (upper panel) and deep (lower panel) water cores from the Chatham Rise and Bounty Trough (Right Panel). Error bars are the combined uncertainties of the calendar age model and $\Delta^{14}C$. The offset between the modern atmosphere and the modern ocean are indicated by the vertical red bars. The panel shading indicates the late glacial (red) and early deglacial (yellow).

4 Discussion

4.1 Timing of Last Episode of Pockmark Formation

A central tenant of our hypothesis is that pockmarks formed at glacial terminations. Here we consider glacial terminations to represent the time period spanning when the Earth's climate reached a minimum temperature (often referred to as Glacial Maxima) and the onset of warming that accompanied the actual deglaciation. In this context, the last glacial termination spans the interval of time between about 30kyBP and ~16kyBP. This is an important distinction because there were many events centered on this time period that cannot be simply classified as either the Last Glacial Maximum (LGM) or the deglaciation. Evidence presented in this study illustrates that $\Delta^{14}C$ began to decrease at sites on the Chatham Rise

and Bounty Trough near 25kyBP (Figure 6). The well-dated Kawakawa tephra was also deposited at 25.6kyBP (Lowe *et al.*, 2013; Sikes and Guilderson, 2016). Atmospheric $\Delta^{14}C$ also began to decrease at this time (Figure 6). In another study, Stott et al (2019) found that radiocarbon activity values at intermediate depths in the eastern equatorial Pacific also began to decrease at about 25kyBP as they did at a deep water site in the South Atlantic (Skinner *et al.*, 2010).

The precise timing of each pockmark exposed at the surface today cannot be ascertained with the data we currently have. However, there are several lines of evidence that indicate the most recent phase of pockmark formation occurred during the last glacial termination. This includes the contrasting ^{14}C and $\delta^{18}O$ stratigraphies from biogenic carbonates deposited within pockmarks (above the base of a pockmark horizon) compared to the isotope stratigraphies from cores collected outside of, but adjacent to pockmarks. To illustrate this, we selected two cores collected from within one of the pockmarks (Figure 7). The ^{14}C age stratigraphy of the bulk inorganic carbon is shown cores PC45 and PC54. Both cores exhibit a dramatic increase in age below 136cm. The PC45 core contains the Kawakawa tephra at 135cm (Figure 7). The ^{14}C ages at 136cm, immediately below the tephra, are radiocarbon dead, implying that there is a hiatus of missing sediment just below the 25.6kyBP tephra horizon. The first sediments to be deposited within the pockmark coincide with the tephra itself and therefore, it appears that this pockmark formed at the time of the Kawakawa Tephra, 25.6kyBP. There is an ongoing effort to conduct similar dating of sediments within the most recent pockmarks to verify the timing of sediments that first filled the pockmarks after they formed.

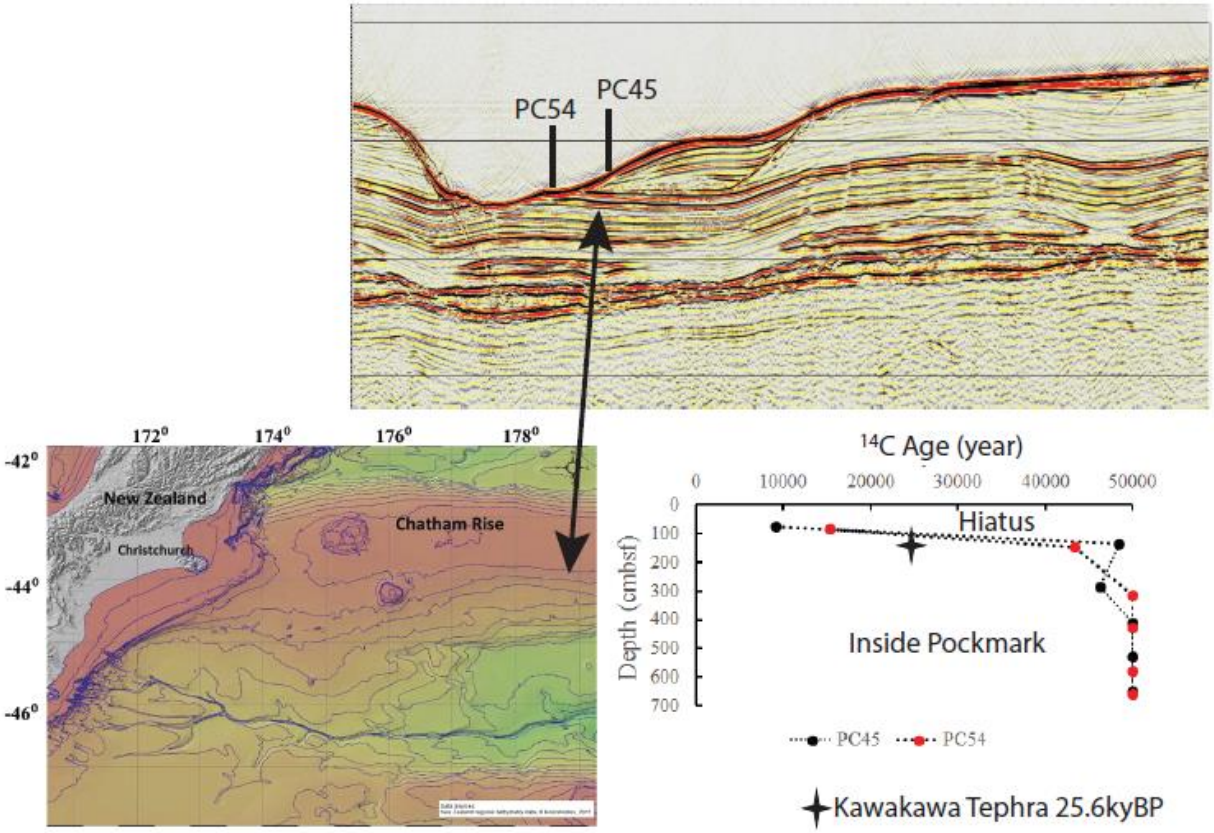

Figure 7. ^{14}C ages of bulk sediment (lower right panel) from two cores collected from a pockmark (upper right panel) on the Chatham Rise. Note the dramatic increase in age just below the Kawakawa tephra in PC45, marking a hiatus of missing sediment that was lost when the pockmark formed just prior to the deposition of the tephra at 25.6kyBP.

4.2 Source of ^{14}C-Depleted Carbon

We have shown that the biogenic sediments that were deposited adjacent to the larger pockmarks on the Chatham Rise and Bounty Trough document large negative $\Delta\Delta^{14}C$ anomalies during the last glacial termination beginning at ~25kyBP that are not observed at other sites near the Chatham Rise. And while it will be important to determine the extent of these radiocarbon anomalies at various depths and at other sites across the Chatham Rise, Rose et al (2010) and Sikes et al (2016) found no large $\Delta\Delta^{14}C$ excursion at shallow intermediate water depths in the Bay of Plenty. We take this initial set of observations to indicate the excursions were restricted to sites on the Chatham Rise and Bounty Trough

where there are large pockmarks above the subsurface conduits. We also find that there is no $\delta^{13}C$-depleted biogenic carbonate accompanying the $\Delta^{14}C$ excursions that would be indicative of methane or petroleum carbon oxidation. When these isotope data are combined with the seismic data it is clear that over-pressurized fluids released from subsurface reservoirs would be the most plausible source of carbon with these geochemical characteristics. If 'old' respired carbon from a formally isolated water mass had been responsible for the depleted $\Delta^{14}C$ values observed in the benthic records, those waters would have also carried a distinctly depleted $\delta^{13}C$ DIC signature, which is not observed (Figure 5). Similarly, if the source of carbon responsible for the depleted $\Delta^{14}C$ values had come from release of methane-rich fluids, that too would have carried a distinctly depleted $\delta^{13}C$ value, which is not observed in the biogenic records. The porewater geochemical profiles at 20 other locations across the study region are all consistent with that of PC75 and PC83 (Coffin *et al.*, 2013b). The extremely low rates of methane flux inferred from the sulfate profiles at all core sites and the lack of any negative $\delta^{13}C$ excursions observed in the biogenic carbonates deposited during the most recent phase of pockmark formation is not consistent with a methane gas source.

Based on the large negative $\Delta^{14}C$ anomaly and lack of a negative $\delta^{13}C$ excursion at the last glacial termination, the most plausible source of carbon would be CO_2 from dissociated limestones at depth beneath the Rise. This is the same carbon source that forms liquid CO_2 that vents today in the western Pacific on Mariana hydrothermal vent system (Lupton *et al.*, 2006). But on the Chatham Rise and Bounty Trough there are no hydrothermal vents. Dissociated carbonates from the subducted Hikurangi Plateau would form buoyant CO_2 that would migrate upward though the fault systems towards the surface.

The depth of the underlying flat-subducted Hikurangi beneath the Chatham Rise and Bounty Trough is largely unknown but is expected to be somewhere between 8 and 20 km. With an average temperature gradient of 40°C/km this implies a temperature between 320^{o}C

and 800°C for the top of the underlying plateau. Dissociation of carbonate is a balance between CO_2 concentration and temperature (Stanmore and Gilot, 2005). At lower temperatures the rate of dissociation is lower and depends on the rate removal of existing CO_2 along faults. Importantly, there has been a massive amount of limestone subducted beneath the Chatham Rise and Bounty Trough for 100 million years. The dissociation rate may be small, but the time for accumulation of dissociated CO_2 is large. There has also been an ongoing history of volcanism along the Chatham Rise since the Cretaceous (Wood and Herzer, 1993). Increased temperatures associated with volcanism will have enhanced CO_2 release. It may also facilitate release of stored CO_2 at depth. Notably, the large volcanic Kawakawa tephra was deposited across the Chatham Rise 25.6kyBP (Lowe *et al.*, 2013; Sikes and Guilderson, 2016) just as the large $\Delta^{14}C$ excursion began (Figure 6).

The very large negative $\Delta^{14}C$ excursion documented by Ronge et al., (2016) from sediments cores taken at the deeper water depths within the Bounty Trough are also adjacent to one of the giant pockmarks (Figure 5). Ronge et al originally called upon transport of ^{14}C-dead carbon from hydrothermal systems located on the East Pacific Rise (EPR) to explain the excursion seen in their Bounty Trough cores. Using a 1-D box model and upscaling, Ronge et al (2016) estimated that a ^{14}C-dead CO_2 flux of 0.16 GtC/yr is required to decrease the entire Southwest Pacific (40-60ºS, 110-180 ºW) $\Delta\Delta^{14}C$ by ~500‰, as observed in their PS75/059-2 record on the EPR and PS75/100-2 on Chatham Rise. However, given the long duration of the $\Delta^{14}C$ excursion it seems likely that ocean mixing would have diluted such a signal by the time it reached the Chatham Rise. This mixing process is missing in Ronge et al's approach. To take this effect into account and to evaluate the impact of ^{14}C-dead DIC flux from the EPR at Chatham Rise, we conducted independent experiments using an Earth System Model of intermediate complexity (cGENIE) (Methods). Although cGENIE is a relatively low-resolution model, it is a suitable tool to evaluate basin-scale radiocarbon budgets over

timescales of several thousand years. In these experiments, a range of ^{14}C-dead DIC between 0.16 to 1.28 GtC/yr was released directly into a 10° by 11°, ~570m thick (3008-3575m) grid box overlying the EPR, where Ronge et al's PS75/059-2 core is located. Deep ocean stratification is enhanced in these simulations through brine rejection in the Southern Ocean (see Methods). This is a relatively crude approach, but we are not intending to match all the observations that constrain the 'LGM' state. Rather, the focus here is how the radiocarbon field in the SW pacific responds to ^{14}C-Dead DIC input from the EPR under a stronger stratification state. For an injection rate of 0.16 GtC/yr as called for by Ronge et al, the magnitude of the simulated $\Delta\Delta^{14}$C excursion in the injected grid box on EPR only reaches 250‰ (Figure 4, blue), not 500‰ as simulated by their 1-box model. The observed ~400‰ decrease in $\Delta\Delta^{14}$C on EPR

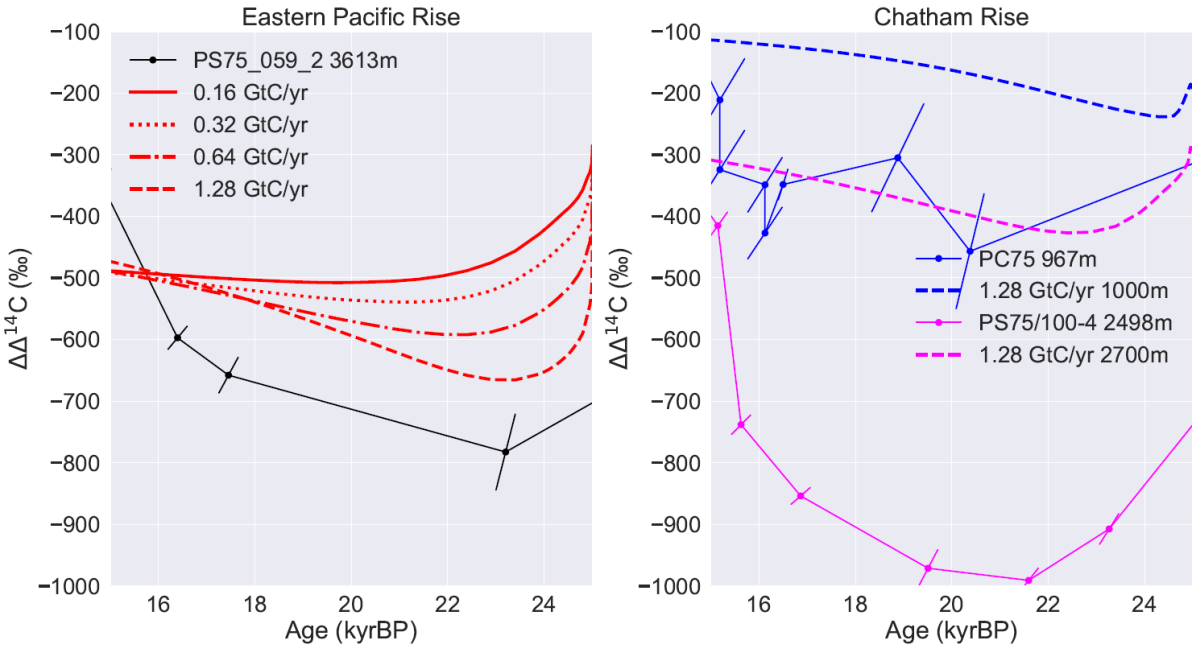

Figure 8. Left panel, red lines represent simulated Δ^{14}C difference between the grid box where ^{14}C-dead DIC was injected and atmosphere ($\Delta\Delta^{14}$C) at different injection rates; the black solid line denotes the PS75-059-2 record (Ronge *et al.*, 2016; Ronge *et al.*, 2019) Right panel, simulated $\Delta\Delta^{14}$C response at ~1000m (the blue dash line) and ~2700m (the purple dash line) on Chatham Rise (CR) under the most extreme DIC injection rate scenario (1.28 GtC/yr); the blue and purple solid line represent the PC75 (this study) and PS75/100-4 (Ronge *et al.*, 2016) record, respectively.

is achieved only in a simulation with an injection rate of 1.28 GtC/yr (Figure 8, left panel, the red curve). However, even in this extreme injection scenario, the simulated $\Delta\Delta^{14}$C change on

Chatham Rise at 2700m (close to Ronge's PS75/100-2) is no larger than 150‰ (Figure 8, right panel), far smaller than is observed in the reconstructed $\Delta^{14}C$ records (Figure 6). And importantly, this small transient reduction in $\Delta\Delta^{14}C$ is not the result of anomalously old ^{14}C from the EPR. Rather, it is caused by the reduced ventilation invoked in the model experiment by enhancing deep water stratification. Furthermore, there is no negative $\Delta^{14}C$ excursion simulated at the PC75 core location (~1000m) on Chatham Rise. These model results do not support the suggestion that ^{14}C -dead DIC can be transported from hydrothermal systems as far away as the EPR to produce the large excursions observed on the Chatham Rise. It is also important to emphasize that mantle-derived CO_2 carries a ^{13}C-depleted signature of ~ -5 to -7‰ (Deines, 2002). There is no negative excursion in benthic $\delta^{13}C$ in association with the $\Delta^{14}C$ excursions on Chatham Rise (Figure 3). Together, the model and observational results presented here make clear that a release of ^{14}C -dead carbon at any single point in the ocean on the EPR or elsewhere will be diluted within a relatively short distance. This means that the large $\Delta^{14}C$ anomalies observed on the Chatham Rise must have come from local sources. The subsurface conduits beneath the pockmarks represent the path those carbon-rich fluids would have taken to the surface. Dissociated Mesozoic carbonate at depth is the most plausible source of that carbon because it would provide ^{14}C-dead carbon and leave no $\delta^{13}C$ anomaly consistent with the data. One of the open questions that remains is whether there was carbonate dissolution upon release of the carbon-rich fluids to the overlying ocean. The most obvious place to look for evidence of dissolution would be at sites close to the Ronge et al cores where the $\Delta^{14}C$ anomalies are large.

4.3 Potential Valving Mechanism for CO_2 Storage and Release

The specific "valving mechanism" for CO_2 accumulation and release, and the formation mechanism for pockmarks at the surface, remains a mystery. The seismic

observations imply the valving mechanism must regulate storage and release of CO_2-rich fluids beneath the sea floor on a regular recurring frequency. With this in mind, several observations point to a link between temperature, sea level and CO_2 hydrate stability that accompanies glacial terminations. The first observation is that the shallowest depth where pockmarks occur on the Chatham Rise (region 1) is at 500m. In the modern ocean the waters at 44ºS and 500m over the Chatham Rise are ~7ºC and thus, ~2ºC below the hydrate stability temperature (Figure 9). Depressurization from sea level change at constant temperature would move the upper limit of pockmark formation near the phase boundary between hydrate and free gas.

There are strong lateral and vertical temperature gradients in these water depths on the Chatham Rise (Figure 9). While sea level changes at temperatures above ~9ºC would have little influence on this phase transition, hydrate stability would be very sensitive to temperature changes. With these factors in mind, there remains many open questions about what may influence hydrate stability. There is a critical need to obtain additional well-resolved records of $\delta^{18}O$ during the last glacial termination from which to develop a better spatial and temporal depiction of when temperatures varied across the Chatham Rise and Bounty Trough. Furthermore, the high solubility of CO_2 requires considerably higher concentrations of CO_2 for formation of CO_2 hydrate than methane for methane hydrate. More accurate knowledge of gas composition is also needed since the addition of small amounts of other gases significantly alters the CO_2-hydrate phase boundary. This information will allow modelling of the predicted movement of top and base of hydrate stability within the sediments through time, specifically accounting for the propagation of temperature signals into the seafloor and the possible thermal sink due to the endothermic nature of hydrate dissociation (Goto *et al.*, 2016). Predicted hydrate dissociation could then be compared to timing of pockmark formation and release of old CO_2 reflected in $\Delta^{14}C$ records.

CO_2 hydrate may have two important roles. It could constitute a near-seafloor ephemeral capacitor, temporally storing CO_2. It may also act as seal inhibiting fluid flow, leading to pressure buildup of CO_2-rich fluids followed by sudden release when the seal dissociates. Ephemeral capacitors unrelated to hydrate could also be present deeper in the sediments: CO_2 could be released from pore waters during depressurization leading to an increase of CO_2 flux towards the seafloor. The role of supercritical CO_2 deeper in the seafloor and variations of its phase boundary following pressure or temperature changes and leading to CO_2 release of uptake will also need to be investigated. From a near-seafloor perspective, these mechanisms would constitute a variation of the source strength for CO_2 flux through glacial cycles, rather than near seafloor storage capacity of CO_2 in the form of hydrate or a temporary seal that dissociates at the end of glacial maxima. These questions motivate our ongoing research.

Whatever the valving mechanism is, it seems evident from the recurrence frequency of

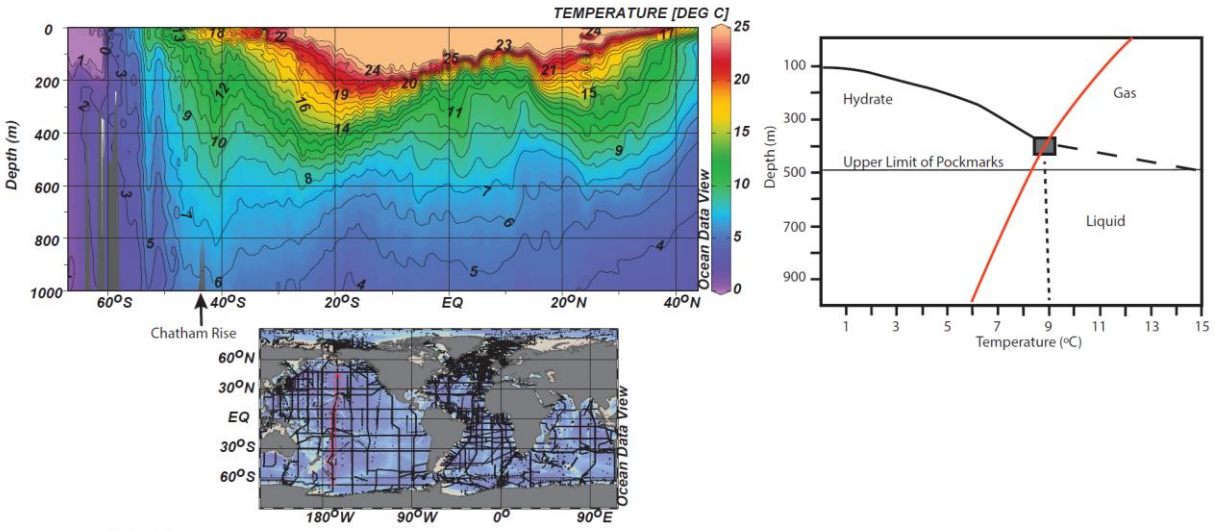

Figure 9. Ocean temperature within the upper 1000m in the Pacific (GLODAP v2) and the three-phase stability of pure CO_2 in seawater. The red line in the right panel is the present-day temperature over the Chatham Rise at 44°S.

pockmarks seen in the seismic sections that CO_2 accumulated over a glaciation and was released rapidly at/near glacial terminations. In this sense the Chatham Rise and Bounty Trough

act as a capacitor for CO_2, analogous to an electrical capacitor that regulates the flux of electrons within a circuit. This intriguing question of what regulates the flow of CO_2 from beneath the Chatham Rise remains an open question and an important topic of ongoing research. Nonetheless, we emphasize that whatever the specific mechanism is that modulates the flux of gas, it is clear that pockmark formation on the Chatham Rise and Bounty Trough has been associated with rapid release of gas and fluids at/near glacial terminations.

The available data cannot be used to estimate how much carbon was released at the last glacial termination from sites on the Chatham Rise. But the magnitude and duration of the $\Delta^{14}C$ excursions imply a sustained release of carbon over several thousand years. If these $\Delta^{14}C$ excursions are seen only at a small number of sites on the Rise, these may not be a significant source of carbon to the ocean at the glacial termination. On the other hand, because of the large number of pockmarks across the Chatham Rise and Bounty Trough (Figure S1) it is reasonable to consider that carbon released from numerous pockmarks on Chatham Rise could have influenced the ocean's carbon budget at the last glacial termination. In this case the release of 'old' carbon may have contributed to the increased reservoir ages of intermediate and surface waters in the southwest Pacific (Rose *et al.*, 2010; Shao *et al.*, 2019; Sikes and Guilderson, 2016; Skinner *et al.*, 2015). Further studies will now be necessary to evaluate whether there were changes in regional carbonate chemistry close to and away from the sites of carbon release.

5 Conclusions

It is increasingly evident that there were several factors influencing the carbon budget of the ocean and the atmosphere simultaneously at the last glacial termination. These likely included some change in the residence time of carbon within the ocean together with geologic processes that include hydrothermal venting (Broecker *et al.*, 2015; Huybers and Langmuir, 2017; Lund *et al.*, 2016; Stott and Timmermann, 2011; Stott *et al.*, 2019) and release of carbon

from subsurface reservoirs such as those beneath Chatham Rise. What is not yet clear however, is how various processes acted in concert with high latitude ocean/atmospheric dynamics to synchronize the glacial cycles of pCO_2 with the orbital variations. Stott and Timmerman (2011) argued that one part of this synchronization may involve temperature changes that are propagated from the Southern Ocean to sites where CO_2 accumulates during glaciations and can be destabilized at glacial terminations. Other studies have argued that a trigger mechanism for release of geologic carbon from hydrothermal systems involves mantle decompression and subsequent invigoration of mantle convection that can promote volcanism (Broecker *et al.*, 2015; Huybers and Langmuir, 2017; Lund and Asimow, 2011). In the case of Chatham Rise, the mechanism responsible for release of carbon-rich fluids responsible for the pockmarks and the $\Delta^{14}C$ anomalies near the deglaciation is yet unknown, but our results indicate it involved buoyancy driven fluid escape. An ultimate test of our hypothesis awaits deep coring into previous glacial terminations to date the timing of previous pockmark formation. But based solely on the recurrence of pockmarks seen in the seismic records we would conclude that the Chatham Rise must act as a carbon capacitor, charging with CO_2-rich fluids from a subsurface carbon reservoir during glaciations and then releasing the stored carbon to the overlying ocean.

Acknowledgments, Samples, and Data

During this study friend and close colleague Robert Thunell passed. This paper is dedicated to his memory and the important influence he had on the field.

We thank two anonymous reviewers for their thoughtful and helpful evaluations of this work. The authors also express gratitude to Patrick Rafter for helpful discussion and suggestions.

L.S. and J.S. were supported by an NSF grant (MG&G 1558990). Funding for BD, HN and IP was provided by the Royal Society of New Zealand "Marsden" Fund, grant UOA1022.

RC and PR were supported by funds from Department of Energy, National Energy Technology Laboratory Morgantown West Virginia, USA. The R/V SONNE cruise SO-226, led by GEOMAR Helmholtz Centre of Ocean Sciences Kiel, was funded by Federal Ministry of Education and Research, Germany through grant 03G0226A. We thank captains Lutz Mallon and Oliver Meyer with their entire crew for their excellent support.

The pore water geochemical data and bulk sediment radiocarbon ages presented in this paper are archived in the PANGAEA data repository (https://doi.pangaea.de/10.1594/PANGAEA.906048). The benthic foraminiferal radiocarbon data for piston core PC75 are archived at https://doi.org/10.1594/PANGAEA.901237. Multibeam data are archived at http://www.marine-geo.org/tools and https://data.gns.cri.nz/pbe/.

The Parasound seismic reflection data (Figure 3), and the seismic reflection lines for Figures 4a and 4b, Figure 7 and Figure S. 2.4, all in SEGY format and two GMT-format grids of bathymetry in Figures 1 and 2 are freely available on https://shop.gns.cri.nz/Chatham_Rise_Bounty_Trough_data at DOI: 10.21420/DMFH-5593 .

References

Adkins, J. F., McIntyre, K., and Schrag, D. P. (2002), The Salinity, Temperature, and delta 18O of the Glacial Deep Ocean, *Science*, *298*(5599), 1769-1773, doi: 10.1126/science.1076252.

Adkins, J. F., and Schrag, D. P. (2003), Reconstructing Last Glacial Maximum bottom water salinities from deep-sea sediment pore fluid profiles, *Earth and Planetary Science Letters*, *216*(1-2), 109-123.

Adkins, J. F. (2013), The role of deep ocean circulation in setting glacial climates, *Paleoceanography*, *28*(3), 539-561, doi: 10.1002/palo.20046.

Anderson, R. F., Ali, S., Bradtmiller, L. I., Nielsen, S. H. H., Fleisher, M. Q., Anderson, B. E., and Burckle, L. H. (2009), Wind-Driven Upwelling in the Southern Ocean and the Deglacial Rise in Atmospheric CO_2, *Science*, *323*(5920), 1443-1448, doi: 10.1126/science.1167441.

Andreassen, K., Hubbard, A., Winsborrow, M., Patton, H., Vadakkepuliyambatta, S., Plaza-Faverola, A., et al. (2017), Massive blow-out craters formed by hydrate-controlled methane expulsion from the Arctic seafloor, *Science*, *356*(6341), 948-953, doi: 10.1126/science.aal4500.

Basak, C., Fröllje, H., Lamy, F., Gersonde, R., Benz, V., Anderson, R. F., et al. (2018), Breakup of last glacial deep stratification in the South Pacific, *Science*, *359*(6378), 900-904, doi: 10.1126/science.aao2473.

Böttner, C., Berndt, C., Reinardy, B. T. I., Geersen, J., Karstens, J., Bull, J. M., et al. (2019), Pockmarks in the Witch Ground Basin, Central North Sea, *Geochemistry, Geophysics, Geosystems*, *20*(4), 1698-1719, doi: 10.1029/2018gc008068.

Broecker, W., Barker, S., Clark, E., Hajdas, I., Bonani, G., and Stott, L. (2004), Ventilation of the Glacial Deep Pacific Ocean, *Science*, *306*, 1169-1172.

Broecker, W., Clark, E., and Barker, S. (2008), Near constancy of the Pacific Ocean surface to mid-depth radiocarbon-age difference over the last 20 kyr, *Earth and Planetary Science Letters*, *274*(3–4), 322-326, doi: http://dx.doi.org/10.1016/j.epsl.2008.07.035.

Broecker, W. S., Yu, J., and Putnam, A. E. (2015), Two contributors to the glacial CO_2 decline, *Earth and Planetary Science Letters*, *429*, 191-196, doi: http://dx.doi.org/10.1016/j.epsl.2015.07.019.

Bryan, S. P., Marchitto, T. M., and Lehman, S. J. (2010), The release of ^{14}C-depleted carbon from the deep ocean during the last deglaciation: Evidence from the Arabian Sea, *Earth and Planetary Science Letters*, *298*(1-2), 244-254, doi: 10.1016/j.epsl.2010.08.025.

Bull, J. M., Barnes, P. M., Lamarche, G., Sanderson, D. J., Cowie, P. A., Taylor, S. K., and Dix, J. K. (2006), High-resolution record of displacement accumulation on an active normal fault: implications for models of slip accumulation during repeated earthquakes, *Journal of Structural Geology*, *28*(7), 1146-1166, doi: https://doi.org/10.1016/j.jsg.2006.03.006.

Burke, A., and Robinson, L. F. (2012), The Southern Ocean's Role in Carbon Exchange During the Last Deglaciation, *Science*, *335*(6068), 557-561, doi: 10.1126/science.1208163.

Cao, L., Eby, M., Ridgwell, A., Caldeira, K., Archer, D., Ishida, A., et al. (2009), The role of ocean transport in the uptake of anthropogenic CO_2, *Biogeosciences*, *6*, 375-390.

Carter, L., Neil, H. L., and McCave, I. N. (2000), Glacial to interglacial changes in non-carbonate and carbonate accumulation in the SW Pacific Ocean, New Zealand, *Palaeogeography, Palaeoclimatology, Palaeoecology*, *162*(3), 333-356, doi: https://doi.org/10.1016/S0031-0182(00)00137-1.

Cartwright, J. A., and Lonergan, L. (1996), Volumetric contraction during the compaction of mudrocks: a mechanism for the development of regional-scale polygonal fault systems, *Basin Research*, *8*(2), 183-193, doi: 10.1046/j.1365-2117.1996.01536.x.

Coffin, R., Hamdan, L., Plummer, R., Smith, J., Gardner, J., Hagen, R., and Wood, W. (2008), Analysis of methane and sulfate flux in methane-charged sediments from the Mississippi Canyon, Gulf of Mexico, *Marine and Petroleum Geology*, *25*(9), 977-987, doi: https://doi.org/10.1016/j.marpetgeo.2008.01.014.

Coffin, R. B., Hamdan, L., Smith, J. P., Plummer, R., Millholland, L., and Larson, R. (2013a), Spatial Variation in Shallow Sediment Methane Source and Cycling along the Alaskan Beaufort Sea, *Marine Petroleum and Geology*, doi: 10.1016/j.marpetgeo.2013.05.002.

Coffin, R. B., Rose, P. R., Yosa, B., and Millholland, L. (2013b), Geochemical evaluation of climate change on the Chatham Rise, US Naval Research Laboratory, Technical Memorandum.

Coffin, R. B., Osburn, C. L., Plummer, R. E., Smith, J. P., Rose, P. S., and Grabowski, K. S. (2015), Deep Sediment-Sourced Methane Contribution to Shallow Sediment Organic Carbon: Atwater Valley, Texas-Louisiana Shelf, Gulf of Mexico, *Energies*, *8*(3), 1561-1583, doi: https://doi.org/10.3390/en8031561.

Coffin, R. B., Hamdan, L.J., Smith, J.P., Rose, P.S., Plummer, R.E., Yoza, B., Pecher., I. Montgomery, M.T. 2014. . Energies 7, 5332-5356; doi:10.3390/en7085332. (2014), Contribution of Vertical Methane Flux to Shallow Sediment Carbon Pools across Porangahau Ridge, New Zealand, *Energies*, *7*, 5332-5356, doi: 10.3390/en7085332.

Coffin, R. B., L. Hamdan, R. Plummer, J. Smith, J. Gardner, W. T. Wood (2008), Analysis of Methane and Sulfate Flux in Methane Charged Sediments from the Mississippi Canyon, Gulf of Mexico, *Marine and Petroleum Geology*, doi: doi:10.1016/j.marpetgeo.2008.01.014.

Davy, B., Pecher, I., Wood, R., Carter, L., and Gohl, K. (2010), Gas escape features off New Zealand: Evidence of massive release of methane from hydrates, *Geophysical Research Letters*, *37*(21), n/a-n/a, doi: 10.1029/2010GL045184.

Davy, B. (2014), Rotation and offset of the Gondwana convergent margin in the New Zealand region following Cretaceous jamming of Hikurangi Plateau large igneous province subduction, *Tectonics*, *33*(8), 2014TC003629, doi: 10.1002/2014TC003629.

de Mahiques, M. M., Schattner, U., Lazar, M., Sumida, P. Y. G., and Souza, L. A. P. d. (2017), An extensive pockmark field on the upper Atlantic margin of Southeast Brazil: spatial analysis and its relationship with salt diapirism, *Heliyon*, *3*(2), e00257, doi: 10.1016/j.heliyon.2017.e00257.

Deines, P. (2002), The carbon isotope geochemistry of mantle xenoliths, *Earth-Science Reviews*, *58*(3), 247-278, doi: https://doi.org/10.1016/S0012-8252(02)00064-8.

Dickens, G. R., Koelling, M., Smith, D. C., Schieders, L., and Scientists, O. E. (2007), Rhizon Sampling of Pore Waters on Scientific Drilling Expeditions: An Example from the IODP Expeditions 302, Arctic Coring Expedtion (ACEX), *Scientific Drilling*, *4*, 22-25.

Donahue, D. J., Linick, T. W., and Jull, A. J. T. (1990), Isotope-Ration and Background Corrections for Accelerator Mass Spactrometry Radiocarbon Meashrements, *Radiocarbon*, *32*(2), 135-142.

Edwards, N. R., and Marsh, R. (2005), Uncertainties due to transport-parameter sensitivity in an efficient 3-D ocean-climate model, *Climate Dynamics*, *24*(4), 415-433, doi: 10.1007/s00382-004-0508-8.

Feldens, P., Schmidt, M., Mücke, I., Augustin, N., Al-Farawati, R., Orif, M., and Faber, E. (2016), Expelled subsalt fluids form a pockmark field in the eastern Red Sea, *Geo-Mar. Lett.*, *36*(5), 339-352, doi: 10.1007/s00367-016-0451-9.

Gohl, K. (2003), Structure and dynamics of a submarine continent: tectonic-magmatic evolution of the Campbell Plateau (New Zealand) - Report of the RV SONNE cruise SO-169, Projekt CAMP, 17 January to 24 February 2003, *Bremerhaven : Alfred-Wegener-Institut für Polar- und Meeresforschungpp. (Berichte zur Polar- und Meeresforschung ; 457)*.

Goto, S., Matsubayashi, O., and Nagakubo, S. (2016), Simulation of gas hydrate dissociation caused by repeated tectonic uplift events, *J. Geophys. Res. Solid Earth*, *121*, 3200-3219, doi: 10.1002/2015JB012711.

Hain, M. P., Sigman, D. M., and Haug, G. H. (2014), Distinct roles of the Southern Ocean and North Atlantic in the deglacial atmospheric radiocarbon decline, *Earth and Planetary Science Letters*, *394*, 198-208, doi: https://doi.org/10.1016/j.epsl.2014.03.020.

Hillman, J. I. T., Gorman, A. R., and Pecher , I. A. (2015), Geostatistical analysis of seafloor depressions on the southeast margin of New Zealand's South Island — Investigating the impact of dynamic near seafloor processes on geomorphology, *Marine Geology*, *360*, 70-83, doi: https://doi.org/10.1016/j.margeo.2014.11.016.

Hovland, M., and Judd, A. G. (1988), *Seabed pockmarks and seepages: Ispact on geology, biology a. the marine environment*, London et al.: Graham, Trotman.

Hovland, M., Gardner, J. V., and Judd, A. G. (2002), The significance of pockmarks to understanding fluid flow processes and geohazards, *Geofluids*, *2*, 127-136.

Hu, R., and Piotrowski, A. M. (2018), Neodymium isotope evidence for glacial-interglacial variability of deepwater transit time in the Pacific Ocean, *Nature Communications*, *9*(1), 4709, doi: 10.1038/s41467-018-07079-z.

Huybers, P., and Langmuir, C. H. (2017), Delayed CO2 emissions from mid-ocean ridge volcanism as a possible cause of late-Pleistocene glacial cycles, *Earth and Planetary Science Letters*, *457*, 238-249, doi: http://dx.doi.org/10.1016/j.epsl.2016.09.021.

Keigwin, L. D., and Lehman, S. J. (2015), Radiocarbon evidence for a possible abyssal front near 3.1 km in the glacial equatorial Pacific Ocean, *Earth and Planetary Science Letters*, *425*, 93-104, doi: http://dx.doi.org/10.1016/j.epsl.2015.05.025.

Klaucke, I., Sarkar, S., Bialas, J., Berndt, C., Dannowski, A., Dumke, I., et al. (2018), Giant depressions on the Chatham Rise offshore New Zealand – morphology, structure and possible relation to fluid expulsion and bottom currents, *Mar. Geol.*, *399*, 158-169, doi: 10.1016/j.margeo.2018.02.011.

Lowe, D. J., Blaauw, M., Hogg, A. G., and Newnham, R. M. (2013), Ages of 24 widespread tephras erupted since 30,000 years ago in New Zealand, with re-evaluation of the timing and palaeoclimatic implications of the Lateglacial cool episode recorded at Kaipo bog, *Quaternary Science Reviews*, *74*, 170-194, doi: http://dx.doi.org/10.1016/j.quascirev.2012.11.022.

Lund, D. C., and Asimow, P. D. (2011), Does sea level influence mid-ocean ridge magmatism on Milankovitch timescales?, *Geochem. Geophys. Geosyst.*, *12*(12), doi: 10.1029/2011GC003693.

Lund, D. C., Mix, A. C., and Southon, J. (2011), Increased ventilation age of the deep northeast Pacific Ocean during the last deglaciation, *Nature Geoscience*, *4*(11), 771-774, doi: https://doi.org/10.1038/ngeo1272.

Lund, D. C., Asimow, P. D., Farley, K. A., Rooney, T. O., Seeley, E., Jackson, E. W., and Durham, Z. M. (2016), Enhanced East Pacific Rise hydrothermal activity during the last two glacial terminations, *Science*, *351*(6272), 478-482, doi: 10.1126/science.aad4296.

Lupton, J., Butterfield, D., Lilley, M., Evans, L., Nakamura, K.-i., Chadwick Jr., W., et al. (2006), Submarine venting of liquid carbon dioxide on a Mariana Arc volcano, *Geochemistry, Geophysics, Geosystems*, *7*(8), doi: 10.1029/2005gc001152.

Mangini, A., Godoy, J. M., Godoy, M. L., Kowsmann, R., Santos, G. M., Ruckelshausen, M., et al. (2010), Deep sea corals off Brazil verify a poorly ventilated Southern Pacific Ocean during H2, H1 and the Younger Dryas, *Earth and Planetary Science Letters*, *293*(3), 269-276, doi: http://dx.doi.org/10.1016/j.epsl.2010.02.041.

Marchitto, T. M., Lehman, S. J., Ortiz, J. D., Fluckiger, J., and van Geen, A. (2007), Marine Radiocarbon Evidence for the Mechanism of Deglacial Atmospheric CO_2 Rise, *Science*, *316*(5830), 1456-1459, doi: 10.1126/science.1138679.

Menviel, L., Spence, P., Yu, J., Chamberlain, M. A., Matear, R. J., Meissner, K. J., and England, M. H. (2018), Southern Hemisphere westerlies as a driver of the early deglacial atmospheric CO_2 rise, *Nature Communications*, *9*(1), 2503, doi: 10.1038/s41467-018-04876-4.

Passaro, S., Tamburrino, S., Vallefuoco, M., Tassi, F., Vaselli, O., Giannini, L., et al. (2016), Seafloor doming driven by degassing processes unveils sprouting volcanism in coastal areas, *Scientific Reports*, *6*, 22448, doi: 10.1038/srep22448 https://www.nature.com/articles/srep22448#supplementary-information.

Petit, J. R., Jouzel, J., Raynaud, D., Barkov, N. I., Barnola, J. M., Basile, I., et al. (1999), Climate and atmospheric history of the past 420,000 years from the Vostok ice core, Antarctica, *Nature*, *399*(6735), 429-436, doi: 10.1038/20859.

Rafter, P. A., Herguera, J.-C., and Southon, J. R. (2018), Extreme lowering of deglacial seawater radiocarbon recorded by both epifaunal and infaunal benthic foraminifera in a wood-dated sediment core, *Climate of the Past, 14*, 1977, doi: https://doi.org/10.5194/cp-14-1977-2018.

Ridgwell, A., Hargreaves, J. C., Edwards, N. R., Annan, J. D., Lenton, T. M., Marsh, R., et al. (2007), Marine geochemical data assimilation in an efficient Earth System Model of global biogeochemical cycling, *Biogeosciences*, *4*, 87–104, doi: https://hal.archives-ouvertes.fr/hal-00297599.

Ronge, T. A., Tiedemann, R., Lamy, F., Kohler, P., Alloway, B. V., De Pol-Holz, R., et al. (2016), Radiocarbon constraints on the extent and evolution of the South Pacific glacial carbon pool, *Nat Commun*, *7*, doi: 10.1038/ncomms11487.

Ronge, T. A., Sarnthein, M., Roberts, J., Lamy, F., and Tiedemann, R. (2019), East Pacific Rise Core PS75/059-2: Glacial-to-Deglacial Stratigraphy Revisited, *Paleoceanography and Paleoclimatology*, *34*(4), 432-435, doi: 10.1029/2019pa003569.

Rose, K. A., Sikes, E. L., Guilderson, T. P., Shane, P., Hill, T. M., Zahn, R., and Spero, H. J. (2010), Upper-ocean-to-atmosphere radiocarbon offsets imply fast deglacial carbon dioxide release, *Nature*, *466*(7310), 1093-1097, doi: http://www.nature.com/nature/journal/v466/n7310/abs/nature09288.html#supplementary-information.

Seeberg-Elverfeldt, J., Koelling, M., and Schluter, M., et al., (2005), Rhizon in situ sampler (RISS) for pore water sampling from aquatic sediment. , in *230th National Meeting of the American-ChemicalSociety*, pp. U1763-U1764 Meeting Abstract: 1799-GEOC American Chemical Socitey, Washington, DC, .

Shao, J., Stott, L. D., Gray, W. R., Greenop, R., Pecher, I., Neil, H. L., et al. (2019), Atmosphere-Ocean CO_2 Exchange Across the Last Deglaciation from the Boron Isotope Proxy, *Paleoceanography and Paleoclimatology* doi: 10.1029/2018PA003498.

Sikes, E. L., Samson, C. R., Guilderson, T. P., and Howard, W. R. (2000), Old radiocarbon ages in the southwest Pacific Ocean during the last glacial period and deglaciation, *Nature*, *405*(6786), 555-559, doi: https://doi.org/10.1038/35014581.

Sikes, E. L., Cook, M. S., and Guilderson, T. P. (2016), Reduced deep ocean ventilation in the Southern Pacific Ocean during the last glaciation persisted into the deglaciation, *Earth and Planetary Science Letters*, *438*, 130-138, doi: https://doi.org/10.1016/j.epsl.2015.12.039.

Sikes, E. L., and Guilderson, T. P. (2016), Southwest Pacific Ocean surface reservoir ages since the last glaciation: Circulation insights from multiple-core studies, *Paleoceanography*, n/a-n/a, doi: 10.1002/2015PA002855.

Sikes, E. L., Allen, K. A., and Lund, D. C. (2017), Enhanced δ13C and δ18O Differences Between the South Atlantic and South Pacific During the Last Glaciation: The Deep Gateway Hypothesis, *Paleoceanography*, *32*(10), 1000-1017, doi: 10.1002/2017pa003118.

Skinner, L., McCave, I. N., Carter, L., Fallon, S., Scrivner, A. E., and Primeau, F. (2015), Reduced ventilation and enhanced magnitude of the deep Pacific carbon pool during the last glacial period, *Earth and Planetary Science Letters*, *411*(0), 45-52, doi: http://dx.doi.org/10.1016/j.epsl.2014.11.024.

Skinner, L. C., Fallon, S., Waelbroeck, C., Michel, E., and Barker, S. (2010), Ventilation of the Deep Southern Ocean and Deglacial CO_2 Rise, *Science*, *328*(5982), 1147-1151, doi: 10.1126/science.1183627.

Somoza, L., León, R., Medialdea, T., Pérez, L. F., González, F. J., and Maldonado, A. (2014), Seafloor mounds, craters and depressions linked to seismic chimneys breaching fossilized diagenetic bottom simulating reflectors in the central and southern Scotia Sea,

Antarctica, *Global and Planetary Change*, *123*, 359-373, doi: https://doi.org/10.1016/j.gloplacha.2014.08.004.

Stanmore, B. R., and Gilot, P. (2005), Review—calcination and carbonation of limestone during thermal cycling for CO_2 sequestration., *Fuel Processing Technology,*, *86*(16), 1707-1743.

Stott, L., Southon, J., Timmermann, A., and Koutavas, A. (2009), Radiocarbon age anomaly at intermediate water depth in the Pacific Ocean during the last deglaciation, *Paleoceanography*, *24*, doi: 10.1029/2008pa001690.

Stott, L., and Timmermann, A. (2011), Hypothesized Link between Glacial/Interglacial Atmospheric CO_2 Cycles and Storage/Release CO_2-Rich Fluids from the Deep Sea., in *Geophysical Monograph Series: Understanding the Causes, Mechanisms and Extent of the Abrupt Climate Change.*, American Geophysical Union, doi: 10.1029/2010GM001052.

Stott, L. D., Harazin, K. M., and Quintana Krupinski, N. B. (2019), Hydrothermal carbon release to the ocean and atmosphere from the eastern equatorial Pacific during the last glacial termination, *Environmental Research Letters*, *14*(2), 025007, doi: 10.1088/1748-9326/aafe28.

Stuiver, M., and Polach, H. A. (1977), Discussion Reporting of ^{14}C Data, *Radiocarbon*, *19*(3), 355-363, doi: 10.1017/S0033822200003672.

Toggweiler, J. R. (1999), Variation of atmospheric CO_2 by ventilation of the ocean's deepest water, *Paleoceanography*, *14*(5), 571-588, doi: 10.1029/1999PA900033.

Waghorn, K. A., Pecher, I., Strachan, L. J., Crutchley, G., Bialas, J., Coffin, R., et al. (2018), Paleo-fluid expulsion and contouritic drift formation on the Chatham Rise, New Zealand, *Basin Research*, *30*(1), 5-19, doi: doi:10.1111/bre.12237.

Wood, R. A., ; , and Herzer, R. H. (1993), The Chatham Rise, New Zealand, in *South Pacific sedimentary basins*, edited by P. F. E. Ballance, pp. 329-349, Amsterdam: Elsevier.

Zhao, N., Marchal, O., Keigwin, L., Amrhein, D., and Gebbie, G. (2018), A Synthesis of Deglacial Deep-Sea Radiocarbon Records and Their (In)Consistency With Modern Ocean Ventilation, *Paleoceanography and Paleoclimatology*, *33*(2), 128-151, doi: doi:10.1002/2017PA003174.